

# The impact of host resistance on cumulative mortality and the threshold of herd immunity for SARS-CoV-2

José Lourenço<sup>a</sup>, Francesco Pinotti<sup>a</sup>, Craig Thompson<sup>a</sup> & Sunetra Gupta<sup>a</sup>

## Affiliations

<sup>a</sup> Department of Zoology, University of Oxford, Oxford, United Kingdom;

## Abstract

It is widely believed that the herd immunity threshold (HIT) required to prevent a resurgence of SARS-CoV-2 is in excess of 50% for any epidemiological setting. Here, we demonstrate that HIT may be greatly reduced if a fraction of the population is unable to transmit the virus due to innate resistance or cross-protection from exposure to seasonal coronaviruses. The drop in HIT is proportional to the fraction of the population resistant only when that fraction is effectively segregated from the general population; however, when mixing is random, the drop in HIT is more precipitous. Significant reductions in expected mortality can also be observed in settings where a fraction of the population is resistant to infection. These results help to explain the large degree of regional variation observed in seroprevalence and cumulative deaths and suggest that sufficient herd-immunity may already be in place to substantially mitigate a potential second wave.

## Main Text

It has been evident from the outset that the risk of severe disease and death from COVID-19 is not uniformly distributed across all age classes, with the bulk of deaths among the +12 million cases reported worldwide (by 12 July 2020, (1)) occurring among older age classes and those with comorbidities (2, 3). It is further becoming clear that risk of infection is also not uniformly distributed across the population (4–9). T-cell and IgG antibody activity have been reported in non-exposed individuals to SARS-CoV-2, suggesting that resistance to infection may accrue from previous exposure to endemic corona viruses (7, 10, 11). A fraction of the population may also already be intrinsically resistant to infection as a consequence of high functioning innate immunity and such mechanistic reasons as reduced expression of Angiotensin Converting Enzyme 2 (ACE2) (12). Here we present a general framework which can be used to systematically explore the impact of these differences in vulnerability to disease and resistance to infection by SARS-CoV-2 on its epidemiology.

Our model (see **Supplementary Text File**) links two subpopulations (groups 1 and 2) by means of an interaction matrix in which  $\delta$  ( $0 < \delta < 1$ ) specifies the degree of within-group mixing in a subpopulation of proportion  $p$ . Thus, all contacts are within the respective groups (i.e. mixing is fully assortative) when  $\delta = 1$ , and between-group mixing is maximised at  $\delta = 0$ . Random or proportionate mixing occurs when  $\delta = p$ . We define the basic reproduction number ( $R_0$ ) for each group as the fundamental transmission potential of the virus within a homogenous population consisting of members of that group. Rates of loss of infection and immunity are given respectively as  $\sigma$  and  $\gamma$ .

The incidence of deaths can be derived from this general framework by assigning appropriate infection fatality rates to the different subpopulations, and factoring in a delay between infection and death. For SARS-CoV-2, this can be achieved by defining a vulnerable fraction to which deaths are confined (see **Supplementary Text File**). However, since the vulnerable fraction is likely to be small, the level of population-wide immunity required to reverse the growth rate of infections may be expected to remain at  $1 - 1/R_0$ , where  $R_0$  is the basic reproduction number in the general population. By contrast, if a fraction  $p$  of the population is resistant to infection ( $R_{0_1} = 0$ ), the herd immunity threshold (HIT) is given as  $(1 - p)(1 - \frac{1}{R_0}[1/(1 - \frac{(1-\delta)p}{(1-p)})])$ , for all values of  $\gamma$ . This suggests that a wide variation in HIT can be observed depending on the proportion resistant, the  $R_0$  within the non-resistant group and the degree of mixing between resistant and non-resistant groups.

**NOTE:** This preprint reports new research that has not been certified by peer review and should not be used to guide clinical practice.

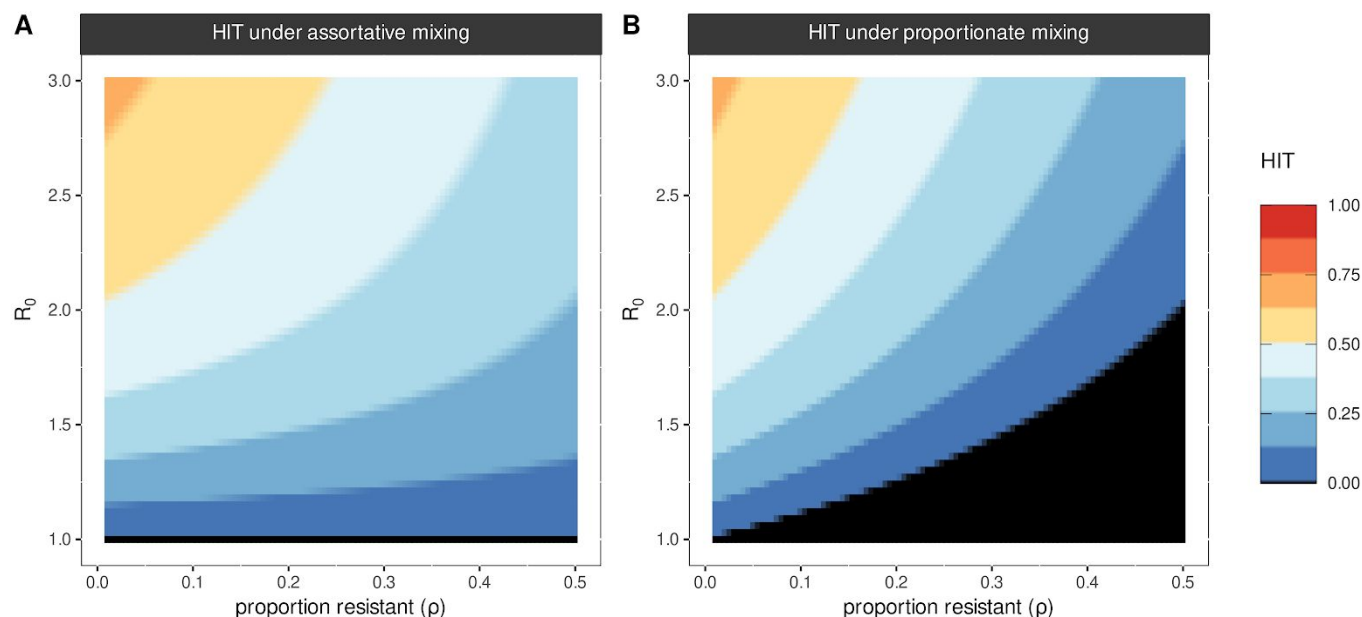


**Figure 1 - Herd-immunity threshold under proportionate and assortative mixing.** Herd-immunity threshold (HIT) when varying proportion of the population fully resistant ( $\rho$ ) under (A) assortative mixing ( $\delta = 1$ ), (B) proportionate mixing ( $\delta = \rho$ ). Each color band equates to a 0.125 change, and black covers the range 0-0.01 ( $R_{01} = 0$ ,  $R_0 = R_{02}$ ,  $1/\sigma = 5$  days,  $\gamma = 0$ ).

	Proportionate mixing					Assortative mixing				
	$R_0 = 1.25$	$R_0 = 1.5$	$R_0 = 2$	$R_0 = 2.5$	$R_0 = 3$	$R_0 = 1.25$	$R_0 = 1.5$	$R_0 = 2$	$R_0 = 2.5$	$R_0 = 3$
$\rho = 0$	0.2	0.33	0.5	0.6	0.66	0.2	0.33	0.5	0.6	0.66
$\rho = 0.1$	0.1	0.23	0.4	0.5	0.56	0.18	0.3	0.45	0.54	0.6
$\rho = 0.2$	0	0.13	0.3	0.4	0.46	0.16	0.26	0.4	0.48	0.53
$\rho = 0.3$	0	0.03	0.2	0.3	0.36	0.14	0.23	0.35	0.42	0.46
$\rho = 0.4$	0	0	0.1	0.2	0.26	0.12	0.2	0.3	0.36	0.4
$\rho = 0.5$	0	0	0	0.1	0.16	0.1	0.16	0.25	0.3	0.33

**Table 1 - Herd-immunity threshold (HIT).** Model output for proportionate mixing ( $\rho = \delta$ , left, light grey) and assortative mixing ( $\delta = 1$ , right, white) for varying basic reproduction number  $R_0$  and proportion resistant  $\rho$ .

When mixing is fully assortative,  $HIT = (1 - \rho)(1 - 1/R_0)$ . In other words, the HIT declines in proportion to the size of the resistant group (**Figure 1A**). For example, when  $R_0 = 2$ , HIT will be reached at 25% if half the population is resistant. By contrast, under proportionate (i.e. random) mixing,  $HIT = 1 - 1/R_0 - \rho$  (**Figure 1B**). This implies that the pathogen will not spread unless the proportion immune is below  $1 - 1/R_0$ . Thus, under the same condition of half the population being resistant, no epidemic will occur unless  $R_0 > 2$ . The dependence of HIT on the degree of within-group mixing ( $\delta$ ) increases with the proportion resistant  $\rho$  (**Figures 2 A & C**), exhibiting their lowest values in a disassortative extreme ( $\delta = 0$ ). We expect that, in most populations, the resistant and non-resistant groups will mix proportionately (represented by the white line in **Figure 2**) but, even in the assortative extreme, the values for HIT we obtain (**Table 1**) are well below those reported by Britton et al (13) in relation to the effects of age and activity structure on HIT. Our results are in broad agreement with those of Gomes et al. (14) under substantial individual variation in susceptibility or connectivity, and the two exercises should be seen to reinforce each other. Our binary approach of resistant versus susceptible with structured mixing has the advantage that we can display the entire range of possible outcomes without needing to explicitly measure the coefficient of variation in susceptibility and exposure to infection. Incomplete resistance can be implemented within this framework by allowing  $R_{01} = F \times R_{02}$  where  $0 < F < 1$  (**Figure S1**); our simulations indicate that under incomplete resistance, the reduction in HIT is roughly proportional to  $F$  (for example,

50% of the population being 50% resistant is roughly equivalent 25% with complete resistance, under proportionate mixing, when  $R_0 = 1.5$ ).

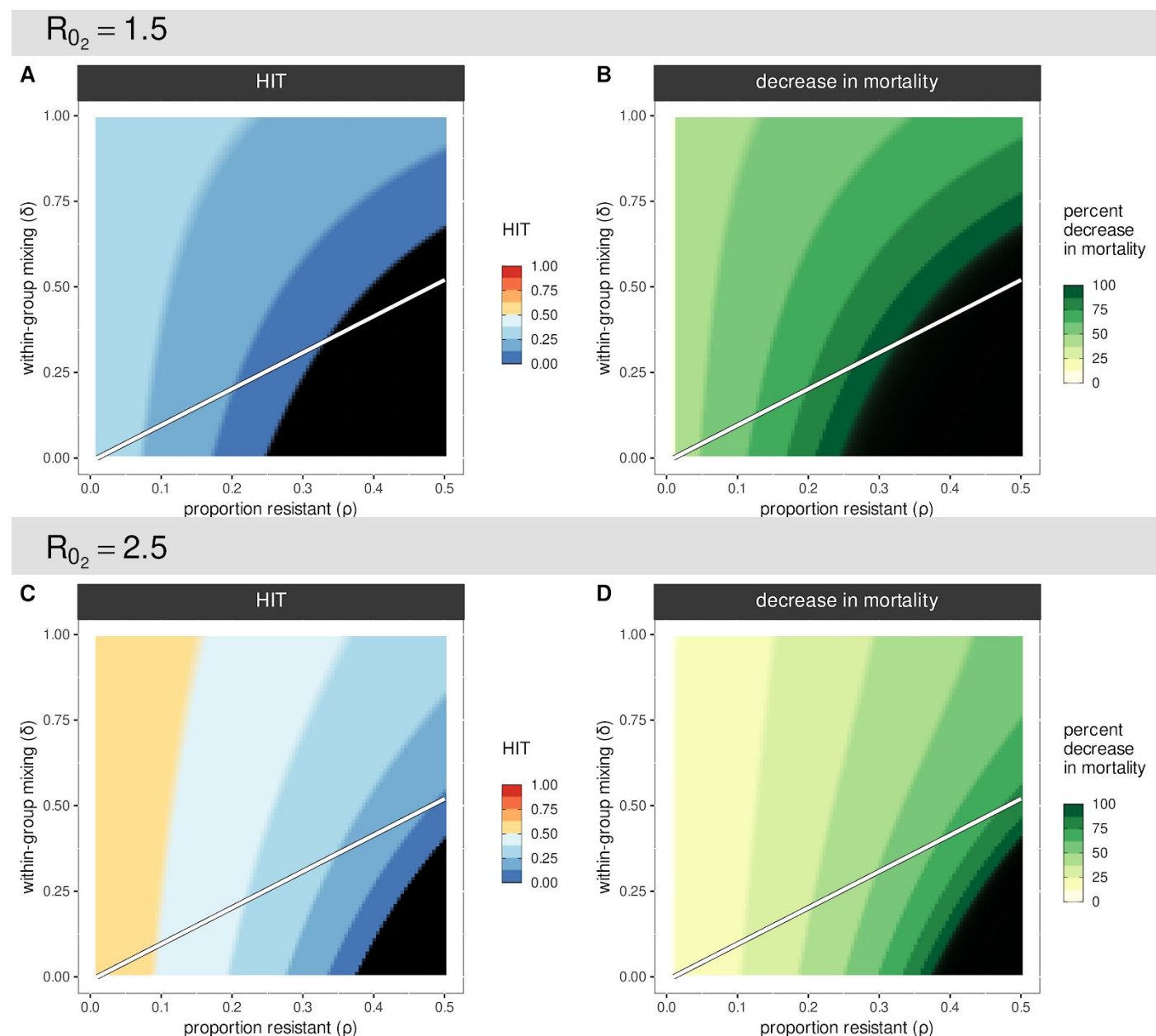


**Figure 2 - Herd-immunity threshold and associated percentage decrease in mortality.** Herd-immunity threshold (A) and percent decrease in mortality (B) for  $R_0 = 1.5$  under different combinations of proportion resistant ( $\rho$ ) and levels of within-group mixing ( $\delta$ ). Panels C and D present the same output but for  $R_0 = 2.5$ . Simulations ran for 365 days with  $1/\sigma = 5$  days,  $\gamma = 0$ ,  $R_{01} = 0$  and  $R_0 = R_{02}$ . Each color band in the color scales equates to a 0.125 change, and black covers the range 0-0.01 in panels A, C and the range 99-100 in panels B, D. For visualisation purposes the percent decrease in mortality is  $100 \times (1 - z/z_{\rho=0})$ , where  $z$  is the proportion exposed at the end of the simulation. The white line designates proportionate mixing ( $\rho = \delta$ ) separating an area of assortative (higher within group) mixing above from disassortative (higher between groups) mixing in the area below.

Maintaining the proportion immune above the threshold of herd immunity prevents the associated pathogen from establishing and spreading within a population. Otherwise, infections will continue to increase until the HIT is reached. Thereafter, the incidence of new infections will fall but the proportion exposed will overshoot HIT and settle eventually at a value often much in excess of HIT (**Figure S2**). Substantial reductions in cumulative mortality can be obtained as the resistant proportion increases (**Figures 2 B & D**) which could provide a simple explanation for the wide variation in death rates reported across various regions.

Provided the proportion of the population exposed is in excess of the HIT, any subsequent epidemic will not occur until the susceptible population is replenished through births and/or loss of immunity. Non-pharmaceutical interventions

preventing the proportion exposed from exceeding the HIT, will leave the population open to further growth in infections once these measures are eased. We further stress that HIT is independent of the rate of loss of immunity ( $\gamma$ ) although the latter will affect the timing and magnitude of the subsequent epidemic peaks (**Figure S3**). Moreover, the public health impact of subsequent peaks will depend on the degree to which previous exposure reduces severity of disease, and not just whether infection-blocking immunity is lost. Given the mounting evidence that exposure to seasonal coronaviruses offers protection against clinical symptoms (9), it would be reasonable to assume that exposure to SARS-CoV-2 itself would confer a significant degree of clinical immunity. Thus, a second peak may result in far fewer deaths, particularly among those with comorbidities in the younger age classes.

Determining the proportion exposed for SARS-CoV-2 is not possible through tracking clinical cases since the majority of infections are likely to be asymptomatic (15), although symptom tracking and other proxies such as excess influenza-like-illness provide a promising alternative route (16, 17). Obtaining these data through serological surveys has proved to be a challenge, principally due to the variability in both antibody and cellular immune responses among exposed individuals and their kinetics (18). Reported levels of seroprevalence have not come close to what people believe to be necessary for herd immunity (18–22). Our results indicate that a wide variation in reported levels of exposure to SARS-CoV-2 can arise as a result of differences in the proportion of the population resistant to infection ( $\rho$ ). High levels of seropositivity can arise under a reasonable range of  $\rho$  and  $R_0$  where HIT is nonetheless lower than the proportion of the population already exposed (**Figure S2**). Equally, seropositivity measures of 10–20% are entirely compatible with local levels of immunity having approached or even exceeded the HIT, in which case the risk and scale of resurgence is lower than currently perceived.

## Supplementary Files

Supplementary Text File - Deriving cumulative deaths from the model by defining a vulnerable fraction to which deaths are confined.

Supplementary Figures - List and legends of supplementary Figures S1–3 (support of main text).

## References

1. World Health Organization, Coronavirus disease (COVID-2019) situation report. *World Health Organization* (2020), (available at <https://www.who.int/emergencies/diseases/novel-coronavirus-2019/situation-reports>).
2. S. Richardson, J. S. Hirsch, M. Narasimhan, J. M. Crawford, T. McGinn, K. W. Davidson, and the Northwell COVID-19 Research Consortium, D. P. Barnaby, L. B. Becker, J. D. Chelico, S. L. Cohen, J. Cookingham, K. Coppa, M. A. Diefenbach, A. J. Dominello, J. Duer-Hefele, L. Falzon, J. Gitlin, N. Hajizadeh, T. G. Harvin, D. A. Hirschwerk, E. J. Kim, Z. M. Kozel, L. M. Marrast, J. N. Mogavero, G. A. Osorio, M. Qiu, T. P. Zanos, Presenting Characteristics, Comorbidities, and Outcomes Among 5700 Patients Hospitalized With COVID-19 in the New York City Area. *JAMA* (2020), doi:10.1001/jama.2020.6775.
3. E. J. Williamson, A. J. Walker, K. Bhaskaran, S. Bacon, C. Bates, C. E. Morton, H. J. Curtis, A. Mehrkar, D. Evans, P. Inglesby, J. Cockburn, H. I. McDonald, B. MacKenna, L. Tomlinson, I. J. Douglas, C. T. Rentsch, R. Mathur, A. Y. S. Wong, R. Grieve, D. Harrison, H. Forbes, A. Schultze, R. Croker, J. Parry, F. Hester, S. Harper, R. Perera, S. J. W. Evans, L. Smeeth, B. Goldacre, OpenSAFELY: factors associated with COVID-19 death in 17 million patients. *Nature* (2020), doi:10.1038/s41586-020-2521-4.
4. Z. Wu, J. M. McGoogan, Characteristics of and Important Lessons From the Coronavirus Disease 2019 (COVID-19) Outbreak in China: Summary of a Report of 72 314 Cases From the Chinese Center for Disease Control and Prevention. *JAMA* (2020), doi:10.1001/jama.2020.2648.
5. Q.-L. Jing, M.-J. Liu, Z.-B. Zhang, L.-Q. Fang, J. Yuan, A.-R. Zhang, N. E. Dean, L. Luo, M.-M. Ma, I. Longini, E. Kenah, Y. Lu, Y. Ma, N. Jalali, Z.-C. Yang, Y. Yang, Household secondary attack rate of

COVID-19 and associated determinants in Guangzhou, China: a retrospective cohort study. *The Lancet Infectious Diseases* (2020), , doi:10.1016/s1473-3099(20)30471-0.

6. N. G. Davies, P. Klepac, Y. Liu, K. Prem, M. Jit, CMMID COVID-19 working group, R. M. Eggo, Age-dependent effects in the transmission and control of COVID-19 epidemics. *Nat. Med.* (2020), doi:10.1038/s41591-020-0962-9.
7. A. Grifoni, D. Weiskopf, S. I. Ramirez, J. Mateus, J. M. Dan, C. R. Moderbacher, S. A. Rawlings, A. Sutherland, L. Premkumar, R. S. Jadi, D. Marrama, A. M. de Silva, A. Frazier, A. F. Carlin, J. A. Greenbaum, B. Peters, F. Krammer, D. M. Smith, S. Crotty, A. Sette, Targets of T Cell Responses to SARS-CoV-2 Coronavirus in Humans with COVID-19 Disease and Unexposed Individuals. *Cell*. **181**, 1489–1501.e15 (2020).
8. A. Nelde, T. Bilich, J. S. Heitmann, Y. Maringer, H. R. Salih, M. Roerden, M. Lübke, J. Bauer, J. Rieth, M. Wacker, A. Peter, S. Hörber, B. Traenkle, P. D. Kaiser, U. Rothbauer, M. Becker, D. Junker, G. Krause, M. Strengert, N. Schneiderhan-Marra, M. F. Templin, T. O. Joos, D. J. Kowalewski, V. Stos-Zweifel, M. Fehr, M. Graf, L.-C. Gruber, D. Rachfalski, B. Preuß, I. Hagelstein, M. Märklin, T. Bakchoul, C. Gouttefangeas, O. Kohlbacher, R. Klein, S. Stevanović, H.-G. Rammensee, J. S. Walz, SARS-CoV-2 T-cell epitopes define heterologous and COVID-19-induced T-cell recognition, , doi:10.21203/rs.3.rs-35331/v1.
9. T. Sekine, A. Perez-Potti, O. Rivera-Ballesteros, K. Strålin, J.-B. Gorin, A. Olsson, S. Llewellyn-Lacey, H. Kamal, G. Bogdanovic, S. Muschiol, D. J. Wullmann, T. Kammann, J. Enggård, T. Parrot, E. Folkesson, O. Rooyackers, L. I. Eriksson, A. Sönnernborg, T. Allander, J. Albert, M. Nielsen, J. Klingström, S. Gredmark-Russ, N. K. Björkström, J. K. Sandberg, D. A. Price, H.-G. Ljunggren, S. Aleman, M. Buggert, Karolinska COVID-19 Study Group, Robust T cell immunity in convalescent individuals with asymptomatic or mild COVID-19, , doi:10.1101/2020.06.29.174888.
10. B. J. Meckiff, C. Ramírez-Suástegui, V. Fajardo, S. J. Chee, A. Kusnadi, H. Simon, A. Grifoni, E. Pelosi, D. Weiskopf, A. Sette, F. Ay, G. Seumois, C. H. Ottensmeier, P. Vijayanand, Single-cell transcriptomic analysis of SARS-CoV-2 reactive CD4 T cells. *bioRxiv* (2020), doi:10.1101/2020.06.12.148916.
11. N. L. Bert, N. Le Bert, A. T. Tan, K. Kunasegaran, C. Y. L. Tham, M. Hafezi, A. Chia, M. Chng, M. Lin, N. Tan, M. Linster, W. N. Chia, M. I.-C. Chen, L.-F. Wang, E. E. Ooi, S. Kalimuddin, P. A. Tambyah, J. G.-H. Low, Y.-J. Tan, A. Bertoletti, Different pattern of pre-existing SARS-COV-2 specific T cell immunity in SARS-recovered and uninfected individuals, , doi:10.1101/2020.05.26.115832.
12. P. Verdecchia, C. Cavallini, A. Spanevello, F. Angeli, The pivotal link between ACE2 deficiency and SARS-CoV-2 infection. *Eur. J. Intern. Med.* **76**, 14–20 (2020).
13. T. Britton, F. Ball, P. Trapman, A mathematical model reveals the influence of population heterogeneity on herd immunity to SARS-CoV-2. *Science* (2020), doi:10.1126/science.abc6810.
14. M. G. M. Gomes, R. M. Corder, J. G. King, K. E. Langwig, C. Souto-Maior, J. Carneiro, G. Goncalves, C. Penha-Goncalves, M. U. Ferreira, R. Aguas, Individual variation in susceptibility or exposure to SARS-CoV-2 lowers the herd immunity threshold. *medRxiv* (2020), doi:10.1101/2020.04.27.20081893.
15. A. Hoxha, C. Wyndham-Thomas, S. Klammer, D. Dubourg, M. Vermeulen, N. Hammami, L. Cornelissen, Asymptomatic SARS-CoV-2 infection in Belgian long-term care facilities. *Lancet Infect. Dis.* (2020), doi:10.1016/S1473-3099(20)30560-0.
16. J. D. Silverman, N. Hupert, A. D. Washburne, Using influenza surveillance networks to estimate state-specific prevalence of SARS-CoV-2 in the United States. *Sci. Transl. Med.* (2020), doi:10.1126/scitranslmed.abc1126.
17. C. Menni, C. H. Sudre, C. J. Steves, S. Ourselin, T. D. Spector, Quantifying additional COVID-19



symptoms will save lives. *Lancet*. **395**, e107–e108 (2020).

18. D. Stadlbauer, J. Tan, K. Jiang, M. Hernandez, S. Fabre, F. Amanat, C. Teo, G. A. Arunkumar, M. McMahon, J. Jhang, M. Nowak, V. Simon, E. Sordillo, H. van Bakel, F. Krammer, Seroconversion of a city: Longitudinal monitoring of SARS-CoV-2 seroprevalence in New York City, , doi:10.1101/2020.06.28.20142190.
19. M. Pollán, B. Pérez-Gómez, R. Pastor-Barriuso, J. Oteo, M. A. Hernán, M. Pérez-Olmeda, J. L. Sanmartín, A. Fernández-García, I. Cruz, N. Fernández de Larrea, M. Molina, F. Rodríguez-Cabrera, M. Martín, P. Merino-Amador, J. León Paniagua, J. F. Muñoz-Montalvo, F. Blanco, R. Yotti, ENE-COVID Study Group, Prevalence of SARS-CoV-2 in Spain (ENE-COVID): a nationwide, population-based seroepidemiological study. *Lancet* (2020), doi:10.1016/S0140-6736(20)31483-5.
20. S. Stringhini, A. Wisniak, G. Piumatti, A. S. Azman, S. A. Lauer, H. Baysson, D. De Ridder, D. Petrovic, S. Schrempft, K. Marcus, S. Yerly, I. Arm Vernez, O. Keiser, S. Hurst, K. M. Posfay-Barbe, D. Trono, D. Pittet, L. Gétaz, F. Chappuis, I. Eckerle, N. Vuilleumier, B. Meyer, A. Flahault, L. Kaiser, I. Guessous, Seroprevalence of anti-SARS-CoV-2 IgG antibodies in Geneva, Switzerland (SEROCoV-POP): a population-based study. *Lancet* (2020), doi:10.1016/S0140-6736(20)31304-0.
21. C. Thompson, N. Grayson, R. Paton, J. Lourenço, B. Penman, L. N. Lee, V. Odon, J. Mongkolsapaya, S. Chinnakannan, W. Dejnirattisai, M. Edmans, A. Fyfe, C. Imlach, K. Kooblall, N. Lim, C. Liu, C. Lopez-Camacho, C.-A. McNally, N. Ramamurthy, J. Ratcliff, P. Supasa, B. Wang, A. J. Mentzer, M. Turner, C. Semple, J. K. Baillie, H. Harvala, G. Screaton, N. Temperton, P. Klenerman, L. Jarvis, S. Gupta, P. Simmonds, ISARIC4C Investigators, Neutralising antibodies to SARS coronavirus 2 in Scottish blood donors - a pilot study of the value of serology to determine population exposure, , doi:10.1101/2020.04.13.20060467.
22. E. Percivalle, G. Cambiè, I. Cassaniti, E. V. Nepita, R. Maserati, A. Ferrari, R. Di Martino, P. Isernia, F. Mojoli, R. Bruno, M. Tirani, D. Cereda, C. Nicora, M. Lombardo, F. Baldanti, Prevalence of SARS-CoV-2 specific neutralising antibodies in blood donors from the Lodi Red Zone in Lombardy, Italy, as at 06 April 2020. *Euro Surveill*. **25** (2020), doi:10.2807/1560-7917.ES.2020.25.24.2001031.